Johannes Geiss, Corinne Charbonnel, Hubert Reeves

Manuel Peimbert & Tom Bania

https://doi.org/10.1017/S174392131000390X Published online by Cambridge University Press

Light Elements in the Universe
Proceedings IAU Symposium No. 268, 2009
C. Charbonnel, M. Tosi, F. Primas & C. Chiappini, eds.

doi:10.1017/S174392131000390X

Measurements of ^{3}He in Galactic H II regions and planetary nebulae

T. M. Bania[1], R. T. Rood[2] and D. S. Balser[3]

[1]Department of Astronomy, Boston University
725 Commonwealth Ave., Boston, MA 02215, USA
email: bania@bu.edu

[2]Astronomy Department, University of Virginia
P.O. Box 400325, Charlottesville, VA 22904, USA
email: rtr@virginia.edu

[3]National Radio Astronomy Observatory,
520 Edgemont Rd., Charlottesville, VA 22903
email: dbalser@nrao.edu

Abstract. The cosmic abundance of the ^{3}He isotope has important implications for many fields of astrophysics. We are using the 8.665 GHz hyperfine transition of $^3He^+$ to determine the ^{3}He/H abundance in Milky Way H II regions and planetary nebulae. Here we review the 30 year history of our ^{3}He program, report on its current status, and describe our future plans.

Keywords. Cosmology: cosmological parameters; The Galaxy: abundances, evolution; ISM: abundances, evolution, H II regions; Stars: AGB, post-AGB

1. The ^{3}He Problem

The ^{3}He abundance in Milky Way sources impacts stellar evolution, chemical evolution, and cosmology. The abundance of ^{3}He is derived from measurements of the hyperfine transition of $^3He^+$ which has a rest wavelength of 3.46 cm (8.665 GHz). As with all the light elements, the present interstellar ^{3}He abundance results from a combination of Big Bang Nucleosynthesis (BBN) and stellar nucleosynthesis (Wilson & Rood 1994). We are measuring the ^{3}He abundance in Milky Way H II regions and planetary nebulae (PNe). H II regions are examples of zero-age objects that are young relative to the age of the Galaxy. Their ^{3}He abundances chronicle the results of billions of years of Galactic chemical evolution (GCE). PNe ^{3}He abundances arise from material that has been ejected from low-mass ($M \leqslant 2\,M_\odot$) and intermediate-mass ($M \sim 2$–$5\,M_\odot$) stars. Because the Milky Way ISM is optically thin at centimeter wavelengths, our source sample probes a larger volume of the Galactic disk than does any other light element tracer of GCE. The sample is currently comprised of 60 H II regions and 12 PNe.

The present ^{3}He abundance is an important GCE diagnostic. H II regions sample the result of the chemical evolution of the Milky Way since its formation. The ^{3}He/H abundance ratio is expected to grow with time and to be higher in those parts of the Galaxy where there has been substantial stellar processing. If the ^{3}He yields predicted by standard models of stellar nucleosynthesis (SSN) had been correct then we should have detected extremely strong $^3He^+$ emission in Galactic H II regions (RST: Rood, Steigman, & Tinsley 1976). Our $^3He^+$ experiment would then have taken about two weeks. After 30 years of effort (Rood, Wilson, & Steigman 1979; Bania *et al.* 2007) our observations still yield ^{3}He abundances for H II regions that are inconsistent with these expectations, leading to "The ^{3}He Problem" (Galli *et al.* 1995).

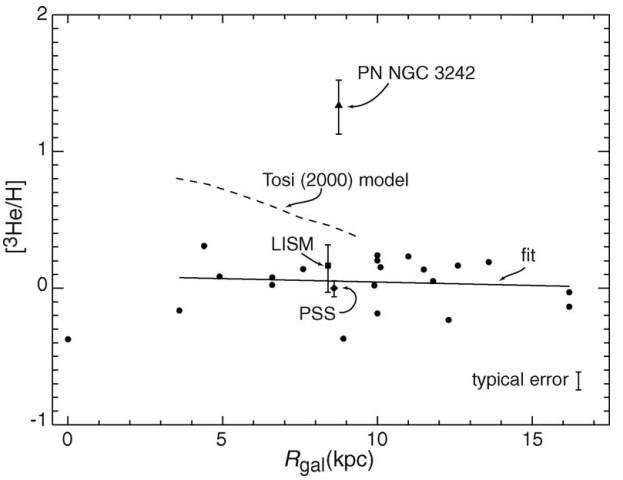

Figure 1. "The ^{3}He Problem" ^{3}He/H abundances as a function of Galactic radius. The [^{3}He/H] abundances by number for the BRB H II region sample are given with respect to the solar ratio. Shown also are the abundances for the planetary nebula NGC 3242 (triangle), the local interstellar medium (LISM—square), and protosolar material (PSS—diamond). There is no gradient in the ^{3}He/H abundance with Galactic position.

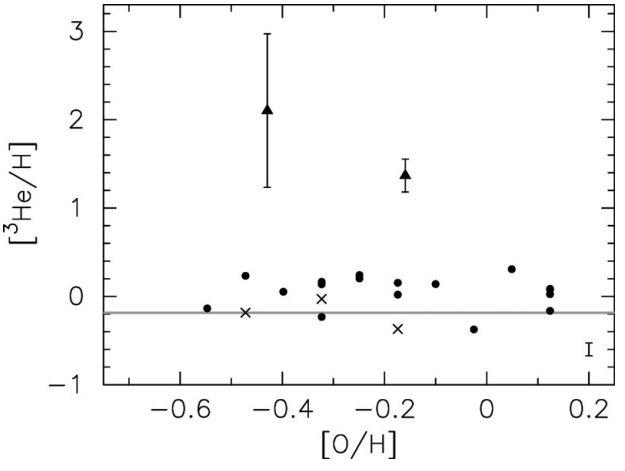

Figure 2. "The ^{3}He Plateau" [^{3}He/H] abundances as a function of source metallicity for the "simple" H II region sample. The gray line is the WMAP result. The ~ 0.15 dex typical error is shown in the right hand corner. The triangles denote abundances for the PNe J 320 (left) and NGC 3242. There is no trend in the ^{3}He/H abundance with source metallicity.

2. H II region abundances

Until its decommissioning in 1999 we used the NRAO 140-Foot telescope to observe $^3He^+$ in a sample of 60 Galactic H II regions (Rood, Bania, & Wilson 1984; Bania, Rood, & Wilson 1987; Balser *et al.* 1994; Rood *et al.* 1995; Bania *et al.* 1997; Balser *et al.* 1999a; Bania, Rood, & Balser 2002; Bania *et al.* 2007). The $\sim 200''$ resolution (FWHM "beam") of the 140-Foot at the $^3He^+$ frequency is comparable to the angular size of typical Galactic H II regions, making this the instrument of choice at the time.

Besides detecting $^3He^+$ emission from an H II region and accurately determining the line intensity and line width, in order to derive the $^3He^+/H^+$ abundance ratio we also need to measure the intensity of the continuum emission produced by thermal free-free

https://doi.org/10.1017/S174392131000390X Published online by Cambridge University Press

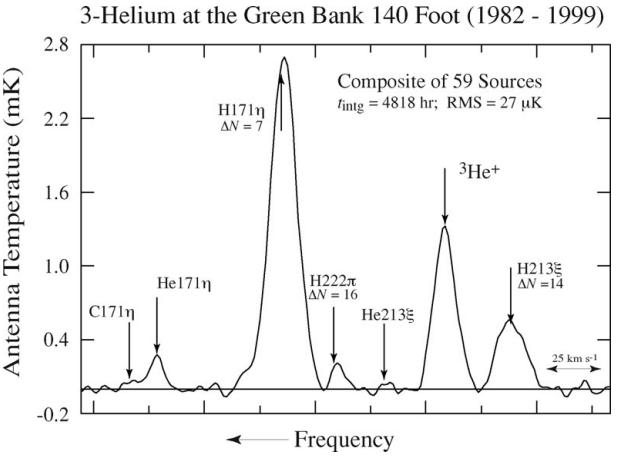

Figure 3. NRAO 140-Foot H II region composite ^{3}He spectrum. This 200 day integration is the most sensitive cm-wavelength spectrum ever taken. Besides the ^{3}He$^+$ emission, a variety of recombination lines from H, ^{4}He, and C are seen. Many of these arise from transitions resulting from large changes in principle quantum number, e.g. H 171 η, Δ N = 7, and H 213 ξ, Δ N = 14.

brehmstrahlung in the nebular plasma. A nebula's ^{3}He$^+$/H$^+$ abundance thus depends on its ^{3}He$^+$ line to thermal continuum intensity ratio. For typical Galactic H II regions the observed line-to-continuum ratio is $\sim 10^{-4}$ to $\sim 10^{-5}$. The 140-Foot's conventional on-axis optics are, moreover, a very poor design for the ^{3}He experiment. Typically, the ^{3}He emission lines have intensities of a few mK and line widths of $\sim$ 1 MHz and this weak, wide line emission must be measured in the presence of the far stronger continuum emission. For conventional blocked aperture optics such as those of the 140-Foot, this strong continuum emission is reflected and scattered by the secondary mirror, its support legs, the receiver cabin, etc., causing direct and multipath standing waves that lead to frequency structure in the observed spectra. This instrumental spectral baseline frequency structure is extremely complex and impossible to model a priori because these standing waves are not pure tones and they vary on short time scales as a source is tracked. Some of the baseline frequency structure can be removed by purposefully defocussing by $\pm\lambda/8$, but much structure remains and needs to be modeled empirically. Baseline modeling errors contribute to the uncertainty in the ^{3}He$^+$ line parameters that we can measure. For H II regions, such errors are too small to compromise our ^{3}He$^+$ detections.

Deriving an accurate ^{3}He/H abundance ratio also requires modeling the nebular density and ionization structure. In doing so we identified a special class of "simple" H II regions for which accurate ^{3}He/H abundances can be determined (Balser *et al.* 1999a). This source sample provides a strong constraint on GCE models. Standard evolution models predict that: (1) the protosolar ^{3}He/H value should be less than that found in the present ISM; (2) the ^{3}He/H abundance should grow with source metallicity; and (3) there should be a ^{3}He/H abundance gradient in the Galactic disk with the highest abundances occurring in the highly-processed inner Galaxy. None of these predictions is confirmed by observations.

Specifically, measurements of ^{3}He/H in protosolar material (Geiss 1993), the local solar neighborhood (Gloecker & Geiss 1996), and Galactic H II regions (Rood *et al.* 1995) all indicate a value of ^{3}He/H $\sim 2 \times 10^{-5}$ by number. Thus the H II regions show no evidence for stellar ^{3}He enrichment during the last 4.5 Gyr. There is no significant ^{3}He abundance gradient across the Milky Way (Fig. 1). And, finally, there is no trend of ^{3}He abundance with source metallicity (Fig. 2). To be compatible with this result GCE

https://doi.org/10.1017/S174392131000390X Published online by Cambridge University Press

models require that $\sim 90\%$ of solar analog stars are non-producers of ^{3}He (Tosi 2000). Finally, BRB argued that the "The ^{3}He Plateau" ^{3}He/H abundance is an upper limit for the cosmological production of ^{3}He. They derived $\eta_{10} = 5.4\ (+2.2/-1.2)$, a year before and in complete concordance with the WMAP value (Spergel *et al.* 2003; Romano *et al.* 2003).

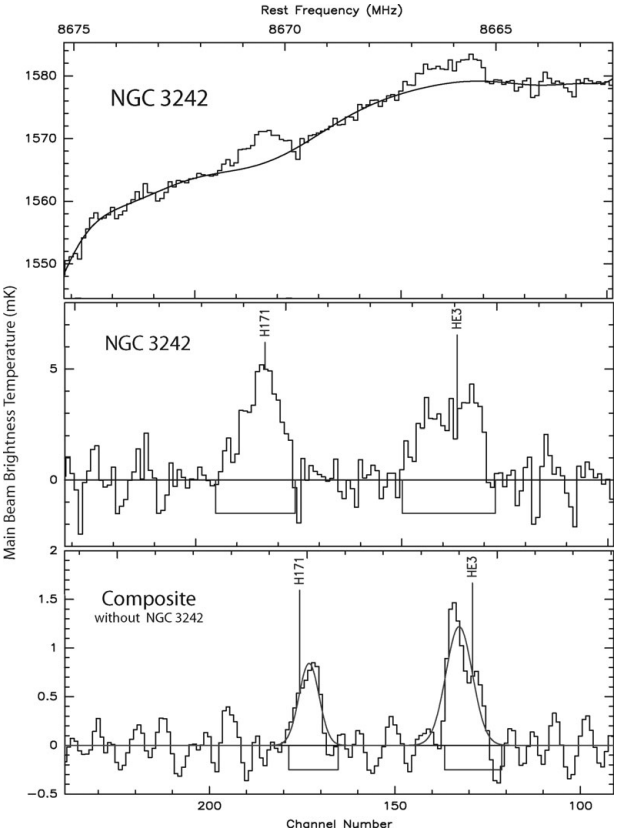

Figure 4. MPIfR 100-m ^{3}He$^+$ spectra for Galactic PNe. **TOP:** The NGC 3242 average spectrum (106 hr integration) with the baseline model superimposed. The H 171 η and ^{3}He$^+$ features are clearly seen. **MIDDLE:** The NGC 3242 spectrum after the baseline model is subtracted. **BOTTOM:** Composite ^{3}He$^+$ average spectrum (443 hr integration) for 6 PNe (NGC 6543, NGC 6720, NGC 7009, NGC 7662, & IC 289).

3. Planetary nebula abundances

Standard stellar evolution theory predicts not only that common solar-type stars produce ^{3}He but also that the mass lost from winds generated at advanced stages of their evolution and the final planetary nebulae should be substantially enriched in ^{3}He. Planetary nebula ^{3}He abundances are therefore important tests of stellar evolution theory since these low-mass, evolved objects are expected to be significant sources of ^{3}He. It is thus crucial to see if stars actually do produce ^{3}He. Detecting ^{3}He$^+$ in the nebulae surrounding PNe is an even more challenging experimental problem than that for H II regions. Finding ^{3}He in PNe challenges the sensitivity limits of all existing radio telescopes. PNe nebulae contain $\sim$1 $M_\odot$ of gas whereas H II region plasmas have masses $\sim$ 100's

https://doi.org/10.1017/S174392131000390X Published online by Cambridge University Press

to ~ 1000's $M_\odot$. The detection of ^{3}He in *any* PN, however, will require $^3\mathrm{He/H} \sim 10^{-4}$, which is the abundance predicted by standard stellar models.

We are observing a sample of 12 PNe that is purposefully biased to maximize the likelihood of finding ^{3}He. Between 1987 and 1997 we used the 100-m telescope of the Max Planck Institut für Radioastronomie (MPIfR) to observe $^3\mathrm{He}^+$ in a sample of 6 PNe (Rood, Bania, & Wilson 1992; Balser *et al.* 1997). The $\sim 85''$ 100-m beam is a good match to the angular extent of typical Galactic PNe. We reported a $^3\mathrm{He}^+$ detection for NGC 3242 and found significant $^3\mathrm{He}^+$ emission in a composite spectrum resulting from the average of 6 PNe (Fig. 4). Even though the continuum emission from PNe is significantly weaker than that from H II regions, the MPIfR optics, which have 22% geometric blockage, produce extremely complex instrumental baseline frequency structure as can be seen in Fig. 4 (top). It was important to verify our $^3\mathrm{He}^+$ detection with another telescope. Despite the fact that PNe with their small angular sizes were not good NRAO 140-Foot targets we were able to verify our NGC 3242 result at the $\sim 4\,\sigma$ level (Fig. 5). The MPIfR and NRAO NGC 3242 line shapes were consistent and they suggested that much of the emission $^3\mathrm{He}^+$ emission comes from a large, diffuse halo. Subsequently we detected $^3\mathrm{He}^+$ emission at the $\sim 4\,\sigma$ level from the PN J 320 with the NRAO Very Large Array (VLA) (Balser *et al.* 2006). It seems that at least *some* (i.e., > 2) PNe produce significant amounts of ^{3}He that survives the PN stage and enriches the ISM.

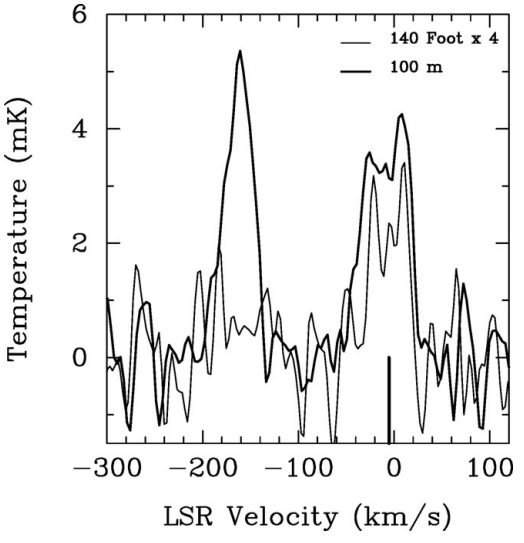

Figure 5. NRAO 140-Foot $^3\mathrm{He}^+$ spectrum for NGC 3242 compared with the MPIfR result. The $^3\mathrm{He}^+$ emission is flagged at $-5.3\,\mathrm{km\,sec}^{-1}$. This 270 hr integration is one of the longest cm-wavelength spectra ever made toward a single source.

4. Current status of the ^{3}He experiment

The $^3\mathrm{He}^+$ experiment challenges the sensitivity limits of all exisiting radio telescope spectrometers. We are now studying ^{3}He with the NRAO Green Bank Telescope (GBT) and NAIC's Arecibo Observatory. We are soon to begin using the NRAO Expanded VLA (EVLA) and ATNF's Parkes 64-m telescope. The EVLA will be a factor of 10 better than the VLA in all relevant experimental parameters. It will be a powerful new tool for studying ^{3}He in PNe. With Parkes it is feasible to detect $^3\mathrm{He}^+$ in the 30 Doradus

https://doi.org/10.1017/S174392131000390X Published online by Cambridge University Press

H II region in the Large Magellanic Cloud. Doing so would extend the metallicity range of the ^{3}He plateau ^{3}He/H abundances.

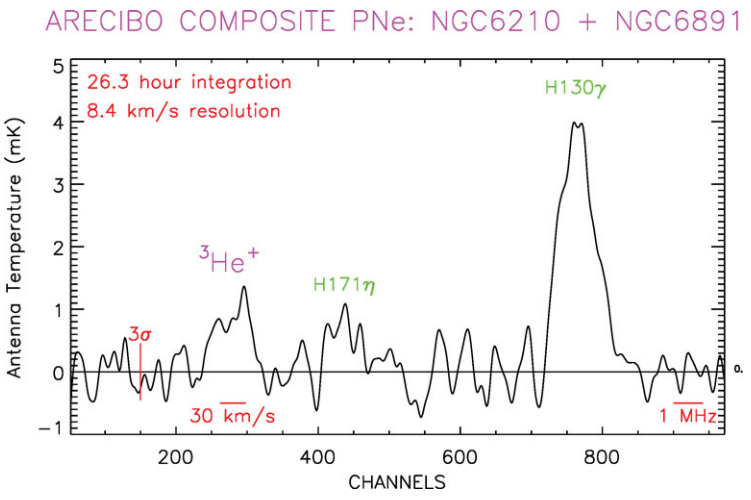

Figure 6. Arecibo ^{3}He$^+$ spectrum for a composite average of 2 Galactic PNe, NGC 6210 & NGC 6891, aligned to a common LSR velocity. A baseline model was removed and the spectrum smoothed to 8.4 km sec^{-1} resolution. The H130γ recombination and ^{3}He$^+$ spin-flip transitions are clearly seen.

We are using the 305-m Arecibo telescope to study ^{3}He$^+$ in PNe. Fig. 6 shows a composite ^{3}He$^+$ spectrum for two PNe. We choose targets to match the properties of the particular telescope we are using. For the most part our Arecibo target PNe were chosen to have angular sizes well matched to its $\sim 45''$ beam. Even though not on our initial Arecibo target list, our VLA results suggested that J 320 was also a plausible target. Thus, to confirm our VLA detection we began observing J 320 in January 2009. At Arecibo we are observing at the high frequency limit set by the surface accuracy of the primary mirror. The primary is fixed in place, which makes Arecibo a semi-transit instrument, so as a source is tracked across the sky different areas of the primary mirror are illuminated. Because of this the telescope gain varies significantly as a source is tracked, which makes intensity calibration difficult. The semi-transit nature of Arecibo also means that progress will be slow. We need significant integration times for our sources, $\sim$ 50–100 hrs, but a full week of observing, 7 sidereal passes of a source, yields 14 hrs of source integration time.

We were part of the 100-m GBT project from its inception through commissioning and are now using it to study ^{3}He$^+$ in H II regions and PNe. Our ^{3}He$^+$ program thus far has focussed on the S 209 H II region and the NGC 3242 PN. Located in the outer Galactic disk at $R_{\rm gal} \sim 16.9$ kpc, S 209 provides an important constraint on BBN and GCE. Confirming the NGC 3242 ^{3}He abundance has important consequences for SSN and GCE. We are also observing the W 3 H II region and the PNe NGC 6543, NGC 6826, and NGC 7009.

The GBT's clear aperture, unblocked optics are unique; it has the potential to be much more sensitive than any cm-wavelength spectrometer ever built. This increased sensitivity results from the 100-m aperture, the unblocked optics, which allow for unprecedented dynamic range, and the unique capabilities of the 3 cm receiver and autocorrelation spectrometer (ACS). For the ^{3}He$^+$ experiment we simultaneously measure 8 different frequency bands at two orthogonal polarizations (RR and LL). Each band is 50 MHz

https://doi.org/10.1017/S174392131000390X Published online by Cambridge University Press

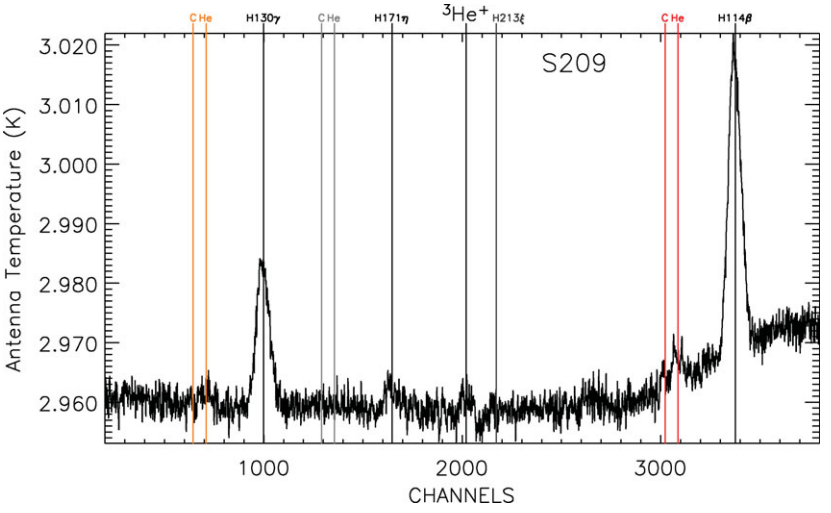

Figure 7. First epoch GBT ^{3}He$^+$ spectrum for H II region S 209. This calibrated, but otherwise unprocessed spectrum, shows that the GBT's unblocked optics have eliminated instrumental standing waves. There is a clear ^{3}He$^+$ signal in this 14.5 hr spectrum. Numerous recombination line transitions of H, and ^{4}He can be seen, including a clear detection of the H 213 ξ line.

wide and is sampled by 4096 channels. We tune two bands to ^{3}He$^+$ in order to assess the GBT's electronics by sampling the identical signal through two independent paths. We thus measure a source's emission over 350 MHz of spectrum (7×50 MHz). The different bands are tuned to a host of radio recombination lines (RRLs) of H, ^{4}He, and C. Our targets' fully ionized plasmas will emit all possible RRL transitions, but at a vast range of intensities. We analyze more than 50 RRL transitions, spanning principal quantum number, N, from 90 through 224 and order, ΔN, from 1 through 16.

As we have done for all the ^{3}He$^+$ experiment telescopes, we use this plethora of RRL measurments to assess the performance of the GBT spectrometer. For example, the RRL line intensities should not vary with time, the ^{4}He/H intensity ratio should not be a function of principle quantum number, and the lines should only be seen in emission. RRL theory predicts line intensities for all these transitions, which can then be used to assess spectrometer performance. For example, in the ^{3}He$^+$ band, LTE models for diffuse H II regions predict that the H 213 ξ intensity should be $\sim 25\%$ the H 171 η intensity (see, e.g., Fig. 3, Fig. 4, & Fig. 5). For any given nebula the entire ensemble of RRLs should give an astrophysically self-consistent set of measured line parameters. Any deviations or inconsistencies are caused by instrumental effects which, experience shows, inevitably appear at some point as one attains ever increasing sensitivity levels. At the sensitivity required by the ^{3}He experiment, characterizing the spectrometer's performance is a on-going, evolving process. We are just now in a position, for example, to begin exploring possible diurnal and seasonal effects on the GBT's instrumental baseline frequency structure.

The current status of the GBT ^{3}He$^+$ experiment for S 209 and NGC 3242 is shown in Fig. 8 (25.8 receiver-hr integration) and Fig. 9 (91.6 receiver-hr integration), respectively. Our GBT ^{3}He$^+$ result for S 209 is completely consistent with our 140-Foot measurement, confirming the ^{3}He/H abundance of "The ^{3}He Plateau."

Extensive analysis of the RRLs from S 209 shows that at our current sensitivity level all spectral features with $\gtrsim 1$ mK intensities are reliably detected. Below this intensity, however, the observed line parameters become uncertain and we begin to see evidence for

https://doi.org/10.1017/S174392131000390X Published online by Cambridge University Press

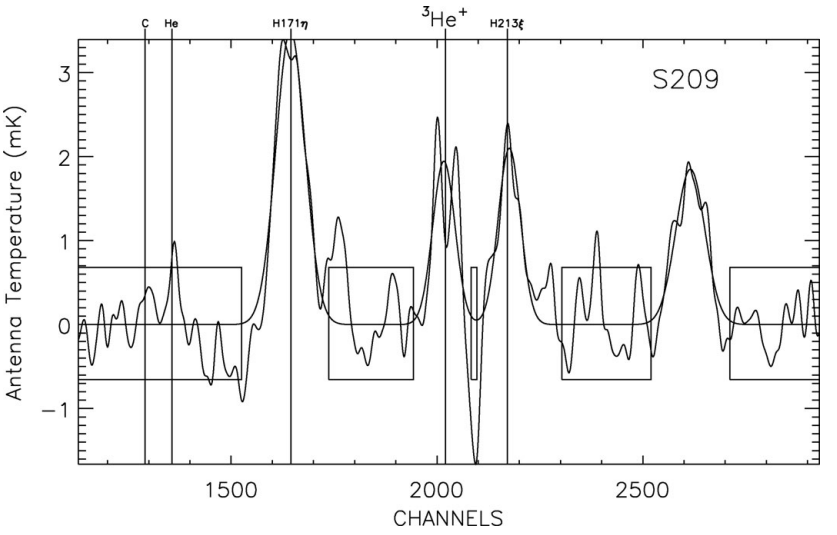

Figure 8. GBT $^3He^+$ average spectrum for H II region S 209 as of November 2009.

instrumental baseline frequency structure (BFS). In the entire 350 MHz spectral range that we measure, we find only a few cases of instrumental BFS that mimic the weak, ~ 1 mK, wide, ~ 1 MHz, lines characteristic of $^3He^+$ emission. Alas, we are very, very unlucky in that the two strongest such instrumental features not only occur within the $^3He^+$ band, but also lie atop the H 213 ξ and H 203 μ RRLs! These instrumental BFS components make the observed H 213 ξ and H 203 μ intensities much too strong (Fig. 8 & Fig. 9). We currently estimate that instrumental BFS enhances these transition intensities by $\sim 20\%$ up to a factor of a few, increasing with source continuum intensity.

Our GBT $^3He^+$ measurements for the PN NGC 3242 (Fig. 9) do not confirm our MPIfR result: the GBT intensities for $^3He^+$ and H 171 η are both lower by a factor of ~ 4. Interestingly, our 140-Foot observations, Fig. 3, also suggested the MPIfR intensities were too high. At the time we attributed the differences between the 100 m and 140-Foot to be due to the different beam sizes: the observed spectra sampled very different volumes surrounding the PN. Density structure, in particular a large, low density, expanding halo could plausibly account for the intensity differences. This can no longer be the case since the GBT and MPIfR beams sizes are essentially identical.

Nonetheless, NGC 3242 *does* have a large, low density, expanding halo which produces a large, ~ 50 km sec^{-1} wide $^3He^+$ line. As can be seen in Fig. 9 this wide $^3He^+$ line blends with the H 213 ξ emission. Moreover, the proximity of H 203 μ, together with the instrumental BFS associated with these RRL transitions makes the $^3He^+$ line parameters uncertain.

We explored a range of baseline models for the NGC 3242 $^3He^+$ emission. Currently, at best, the GBT data are consistent with a $^3He^+$ abundance ratio of $\sim 10^{-4}$ by number, with an uncertainty of $\sim 50\%$. We also studied a variety of composite $^3He^+$ spectra for our GBT PNe sources. The best such cases are consistent with the composite PNe spectra obtained at the MPIfR and Arecibo. Again, these composites are consistent with a $^3He^+$ abundance ratio of $\sim 10^{-4}$ by number.

https://doi.org/10.1017/S174392131000390X Published online by Cambridge University Press

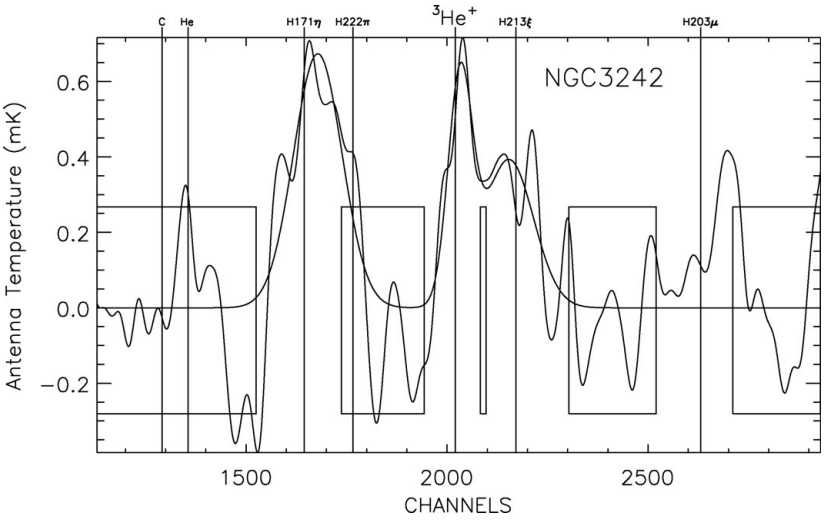

Figure 9. GBT $^3He^+$ average spectrum for NGC 3242 as of November 2009.

5. Solving "The ^{3}Helium Problem"

Rood, Bania, & Wilson (RBW: 1984) suggested that the ^{3}He problem could be related to striking chemical anomalies in red giant stars. Much accumulated observational evidence shows that low-mass RGB stars undergo an extra-mixing event. This extra-mixing adds to the standard first dredge-up to modify the surface abundances. Efforts by many groups during the past 25 years have confirmed that RBW were on the right track. Significantly, all the relevant data indicate that the extra-mixing occurs in $\sim$ 90 to 95% of the low-mass stars. Thermohaline instability and rotation-induced mixing now seem to be able to account for the drastically reduced ^{3}He yields produced by low-mass red giants (Charbonnel & Zahn 2007a,b; Charbonnel & Lagarde 2010; Eggleton, Dearborn, & Lattanzio 2006).

6. Summary

The NRAO GBT result for S 209 is consistent with *all* previous Galactic H II region ^{3}He/H abundance determinations. Thus "The 3-Helium Plateau" ^{3}He/H abundance, important for primordial nucleosynthesis and Galactic chemical evolution, stands. The ^{3}He/H abundance by number, which is not seen to be a function of either source metallicity or Galactic position, is $\sim 2 \times 10^{-5}$.

Attempting to detect ^{3}He in PNe challenges the capabilities of all existing radio spectrometer systems. We reported ^{3}He detections in NGC 3242 with the MPIfR 100 m and NRAO 140-Foot telescopes. Our NRAO GBT observations are, however, inconsistent with the MPIfR 100 m result, implying a ^{3}He/H abundance that is $\sim$ 25% of that we previously reported. We find ^{3}He in J 320 at the $4\,\sigma$ level with the NRAO VLA. Confirmation observations are underway using the NAIC Arecibo telescope. Composite PNe $^3He^+$ spectra, made from MPIfR, Arecibo, and GBT observations, consistently show $^3He^+$ emission at the $\sim$ 1 mK level. As a class our sources imply a ^{3}He/H abundance by number of $\sim 10^{-4}$, which suggests that some PNe produce ^{3}He.

Resolving "The ^{3}He Problem" requires that the vast majority of low-mass stars fail to enrich the ISM with ^{3}He due to extra-mixing in the RGB stage. GCE models can account for "The ^{3}He Plateau" only if $\gtrsim$ 90% of solar analog stars are non-producers of

https://doi.org/10.1017/S174392131000390X Published online by Cambridge University Press

^{3}He. Thermohaline instability and rotation-induced mixing are able to account for the drastically reduced ^{3}He yields produced by these stars. Our PNe target sample is purposefully biased to contain objects whose progenitor stars underwent no extra-mixing, which has been suppressed by some yet to be determined mechanism (but see the conjecture by Charbonnel & Zahn 2007b; Charbonnel & Lagarde 2010). These rare PNe seem to be returning ^{3}He to the ISM.

Acknowledgements

We thank the international light element abundances community for their collegiality and support over the years.

References

Balser, D. S., Bania, T. M., Brockway, C. J., Rood, R. T., & Wilson, T. L. 1994, *ApJ*, 430, 667
Balser, D. S., Bania, T. M., Rood, R. T., & Wilson, T. L. 1997, *ApJ*, 483, 320
Balser, D. S., Bania, T. M., Rood, & Wilson, T. W. 1999, *ApJ*, 510, 759
Balser, D. S., Rood, R. T., & Bania, T. M. 1999, *ApJ*, 522, L73 [N3242]
Balser, D. S., Goss, W. M., Bania, T. M., & Rood, R. T. 2005, *ApJ*, 640, 360 [J320]
Bania, T. M., Balser, D. S., Rood, R. T., Wilson, T. L., & Wilson, T. J. 1997, *ApJS*, 415, 54
Bania, T. M., Balser, D. S., Rood, R. T., Wilson, T. L., & LaRocque, J. M. 2007, *ApJ*, 664, 915
Bania, T. M., Rood, R. T., & Wilson, T. L. 1987, *ApJ*, 323, 30
Bania, T. M., Rood, R. T., & Balser, D. S. 2002, *Nature*, 415, 54
Charbonnel, C. & Zahn, J. P. 2007a, *A&A*, 467, L15
Charbonnel, C. & Zahn, J. P. 2007b, *A&A*, 476, L29
Charbonnel, C. & Lagarde, N. 2010, in: C. Charbonnel, M. Tosi, F. Primas, & C. Chiappini (eds.), *Light Elements in the Universe*. Proc. IAU Symposium No. 268, (Cambridge: CUP), p. XX
Eggleton, P. P., Dearborn, D. S. P., & Lattanzio, J. C. 2006, *Science*, 314, 1580
Galli, D., Palla, F., Ferrini, F., & Penco, U. 1995, *ApJ*, 443, 536
Galli, D., Stanghellini, L., Tosi, M., & Palla, F. 1997, *ApJ*, 456, 478
Geiss, J. 1993, in: N. Prantzos, E. Vangioni-Flam, & M. Casse (eds.), *Origin and Evolution of Elements*. (Cambridge: CUP), p. 89
Gloecker, G. & Geiss, J. 1996, *Nature*, 381, 210
Palla, F., Galli, D., Marconi, A., Stanghellini, L., & Tosi, M. 2002, *ApJ*, 568, L57
Romano, D., Tosi, M., Matteucci, F., & Chiappini, C. 2003, *MNRAS*, 346, 295
Rood, R. T., Bania, T. M., & Wilson, T. L. 1984, *ApJ*, 280, 629
Rood, R. T., Bania, T. M., & Wilson, T. L. 1992, *Nature*, 355, 618
Rood, R. T., Bania, T. M., Wilson, T. L., & Balser, D. S. 1995, in: P. Crane (ed.), *ESO/EIPC Workshop on the Light Elements*. (Heidelberg: Springer), p. 201
Rood, R. T., Steigman, G., & Tinsley, B. M. 1976, *ApJ*, 207, L57 [RST]
Rood, R. T., Wilson, T. L., & Steigman, G. 1979, *ApJ*, 227, L97
Spergel, D. N. *et al.* 2003 *ApJS*, 148, 175
Tosi, M. 2000, in: L. da Silva, M. Spite, & J. R. de Medeiros (eds.), *The Light Elements and Their Evolution*, Proc. IAU Symposium No. 198, (San Francisco: ASP), p. 525
Wilson, T. L. & Rood, R. T. 1994, *ARAA*, 32, 191